The chemical composition of IRAS 05341+0852:
a post-AGB F supergiant with 21 μm emission

B.E. Reddy[1], **M. Parthasarathy**[1,2], **G. Gonzalez**[3,4], **and E.J. Bakker**[3]

[1] Indian Institute of Astrophysics, Bangalore - 560 034, India
[2] Observatoire Astronomique, de Strasbourg, 11 rue de l' Universite, F-67000 Strasbourg, France
[3] Department of Astronomy and McDonald Observatory, University of Texas, Austin, TX 78712, USA
[4] Present address: Astronomy Department, University of Washington, Box 351580, Seattle, WA 98195-1580 USA

Abstract. An abundance analysis of the photosphere of the F-type Post-AGB candidate IRAS 05341+0852 is presented. The analysis of the spectra suggests that the atmospheric model: T_{eff}=6500 K, log g=0.5, ξ_t=5 km s^{-1} and [M/H]=-1.0, best represents the photosphere of the star. We find that the star is metal-poor ([Fe/H]=-0.9) and carbon-rich (C/O$\approx$1.9). Lithium, carbon, nitrogen, oxygen, aluminum and silicon are found to be overabundant. Most importantly this star has large overabundance of s-process elements which are as follows: [Y/Fe]=1.6, [Ba/Fe]=2.2, [La/Fe]=2.9, [Ce/Fe]=1.6, [Pr/Fe]=1.8, [Nd/Fe]=2.0, and [Sm/Fe]=1.7. These s-process enhancements are of similar magnitude to those seen in FG Sge.

The enhancement of Li and Al are expected due to Hot Bottom Burning (HBB), in massive AGB stars. However, the low metallicity, heliocentric radial velocity (v_r = 25 km s^{-1}), and the high Galactic latitude (b = -12°) suggest that IRAS 05341+0852 is a low-mass star. Also the [S/Fe]=0.2 indicates that the low Fe abundance is intrinsic and is not due to fractionation. The significant overabundance of lithium (log $\epsilon \le$ 2.5) and aluminum ([Al/Fe]=1.4) in this star is a puzzle.

Furthermore we have detected the C$_2$ Phillips and CN Red bands in absorption. We find rotational temperatures, column densities, and expansion velocities which show that these lines are formed in the detached circumstellar dust shell (the AGB ejecta) and we find an expansion velocity of the AGB ejecta of v_{exp} = 10.8 $\pm$ 1.0 km s^{-1}.

Key words: stars: abundances – stars: carbon-stars; post-AGB stars; circumstellar matter – stars: individual: IRAS 05341+0852
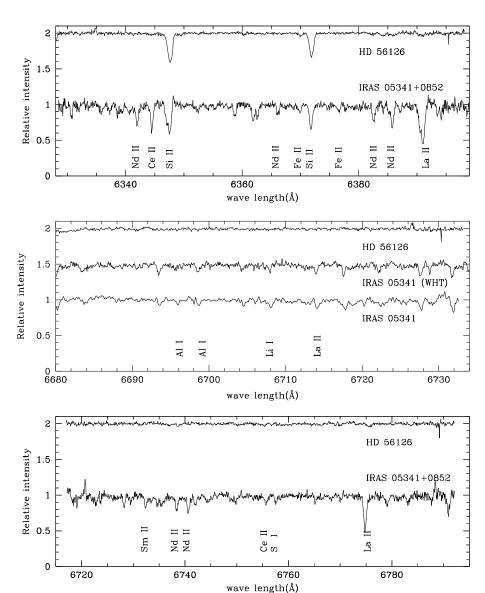
1. Introduction

Asymptotic Giant Branch (AGB) stars, post-AGB stars, and Proto-Planetary Nebulae (PPNe) and PNe which have dust envelopes around them are among the most numerous objects detected by IRAS. These are very luminous infrared objects corresponding to the critical phases of evolution of low- and intermediate-mass stars. Detailed studies of these objects in the wavelength regions from ultraviolet to radio provide clues to understand the role of thermal pulses, nucleosynthesis, mixing, mass-loss, and the transition from oxygen- to carbon-rich stars.

The discovery of dust shells with far-IR colors similar to PNe around some of the bright high latitude A- and F-supergiants and the interpretation that these are post-AGB supergiants (Parthasarathy & Pottasch 1986, Kwok et al. 1987) led to detailed study of these objects. Pottasch & Parthasarathy (1988) have shown that some of these stars have unusual IRAS Low Resolution Spectra. The CO/HCN line ratios of several of these post-AGB stars indicate that they have carbon-rich circumstellar envelopes (Omont et al. 1993). The infrared spectra of some of these post-AGB stars show unidentified infrared features at 3.3, 6.2, 7.7, 8.6, and 11.3 μm, which are commonly attributed to the Polycyclic Aromatic Hydrocarbons (PAH).

Recently, detection of a strong broad emission feature at 21 μm and unusually strong 3.4-3.5 μm and 6-9 μm emission features in several PPNe and post-AGB stars were reported (Kwok et al. 1995 and references therein). The optical spectroscopy has indicated that all the 21 μm emission sources are carbon-rich (Hrivnak 1995, Bakker et al. 1996a,b). Detailed chemical abundance studies of the post-AGB stars HD 56126 (Parthasarathy et al. 1992, Klochkova 1995) and HD 187885 (van Winckel et al. 1996) have shown that both stars are overabundant in carbon and s-process elements indicating that they have gone through the third dredge-up.

Thus, detailed chemical composition analysis of post-AGB stars with carbon-rich photospheres and carbon-rich circumstellar dust permit us to study the correlation between C/O and abundances of s-process elements and the association of s-process enhancements with shell-flashes and dredge-up.

Geballe & van der Veen (1990) suggested that IRAS 05341+0852 (hearafter, IRAS 05341) is an evolved F-type supergiant with carbon-rich circumstellar dust. Parthasarathy (1993) found it to be a F-type supergiant with

Fig. 1. Parts of the spectrum of IRAS 05341 and HD 56126 showing the presence of s-process elements. In the middle panel spectra in the Li I region obtained with WHT and McDonald telescope are displayed. In both the spectra, Li I and Al I lines are clearly seen.

IRAS colours similar to planetary nebulae. Manchado et al. (1989) obtained near-IR photometry of this star. IRAS 05341 shows 3.3, 3.4-3.5,7.7, and 11.3 μ PAH-related emission features (Geballe & van der Veen 1990, Kwok 1995) and also weak 21 μ feature (kwok 1995). Reddy & Parthasarathy (1996) studied the flux distribution and low resolution optical spectrum and concluded that IRAS 05341 is an F6 supergiant star.

In this paper, we report on a detailed chemical composition analysis of the photosphere of IRAS 05341 and examine its circumstellar environment via molecular absorption lines in the optical.

2. Observations

Spectra of high resolving power ($\lambda/\Delta\lambda \approx$ 45,000) of IRAS 05341 and HD 56126 have been obtained in the range 6200-8000 Å (11th December 1996 and 3rd February 1996) and 5470-7200 Å (8th December 1996) respectively, at McDonald observatory with the 2.1 m telescope equipped with the
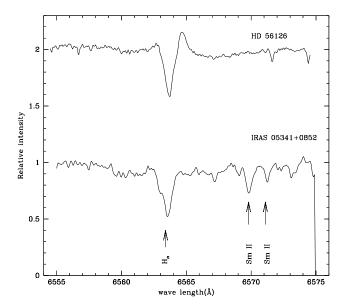
Cassegrain Echelle Spectrograph and a Reticon 1200 × 400 pixel CCD (McCarthy et al. 1993). The S/N ratio of the spectra of IRAS 05341+0852 average near 40. The CCD spectra were reduced using a standard data analysis program (NOAO IRAF).

We have also analyzed the high resolution (45,000) spectra in the Li I doublet at 6707Å and OI triplet at 6156Å regions, obtained with the Utrecht Echelle Spectrograph (UES) on the William Herschel Telescope (WHT) at La Palma. These spectra were obtained by Dr. Hans van Winckel and he has kindly provided them for our use in this analysis.

3. Analysis

3.1. Description of the spectra

A few selected regions of the spectra of IRAS 05341 are compared with those of HD 56126 (Fig. 1). HD 56126 is a F-type post-AGB supergiant with overabundances of carbon and s-process elements (Parthasarathy et al. 1992, Klochkova 1995)

Fig. 2. $H\alpha$-profiles of IRAS 05341+0852 and HD 56126.

It is clear from Fig. 1 that the spectra of IRAS 05341 are completely dominated by s-process elements Nd, Ce, La, Sm, Pr, etc. The heavy element line identifications were done using the spectra of s-process rich star FG Sge (Kipper & Kipper 1993). The Li I ($EW = 38$ mÅ) doublet line at 6707 Å is clearly seen in the spectra of IRAS 05341 (Fig. 1).

We also identified the S I and Al I lines in the spectrum of IRAS 05341 (Fig. 1). The sharp spectral features in IRAS 05341+0852 suggest that the star has a highly extended atmosphere. The $H\alpha$ profile of IRAS 05341 is shown along with that of HD 56126 in Fig. 2. Its $H\alpha$ profile shows emission in the wings and a narrow absorption core indicating an extended atmosphere and mass-loss.

3.2. Atmospheric models and atomic data

Elemental abundances have been derived with the local thermodynamic equilibrium (LTE) model atmosphere grids computed by MARCS code of Gustafsson et al. (1975). We used the updated code "LINES" based on the code "MOOG" developed by Sneden (1973) in deriving the elemental abundances. The method involves measuring the equivalent widths of individual lines, which, when combined with model atmospheres, are used to derive the elemental abundances. The abundances of Li, S, and CNO have been determined from spectrum synthesis analysis allowing for blends.

For the oscillator strengths (gf values), we made use of the recent compilation of R.E. Luck (private communication). The gf values of sulphur are taken from Biemont et al. (1993) and gf values of C, N and O are from Lambert et al. (1982). The gf values for Al I, Ca I, Fe I, Fe II, Ni I, Y II, Ba II, Ce II and Eu II lines (Table 1) are taken from the Thévenin (1989, 1990) solar gf values. The La II abundances are based on the reliable gf values determined recently by Bord et al. (1996).

The gf values for many Nd II lines in our spectral range are not available. Out of many identified Nd II lines we have gf values for only 2 lines, one at 6365.550 Å (Ward 1985), 5842.385 Å (158mÅ) (Thévenin 1989, 1990). The gf values for Sm II and Pr II are taken from Kurucz & Peytremann (1975).

Reddy & Parthasarathy (1996) have estimated effective temperature, $T_{\rm eff}$=6500 K and surface gravity, $\log g = 1.0$ by comparing the flux distribution of this source with Kurucz (1979) atmospheric models. The $B - V$ versus $T_{\rm eff}$ calibration (Flower 1977) yields $T_{\rm eff}$=6200 K. We used these parameters as initial values in deriving the accurate atmospheric parameters.

A spectroscopic estimate of $T_{\rm eff}$ is found by identifying the model atmospheres for which the iron abundance given by Fe I lines is independent of their low excitation potential (LEP). The Fe I lines used in determining $T_{\rm eff}$ have LEP in the range of $2.2 - 4.2$ eV. Log g has been determined by forcing the Fe I and Fe II lines to yield the same iron abundance for the given $T_{\rm eff}$ and ξ_t (micro turbulent velocity). The ξ_t has been determined from individual Fe I lines to show no dependence on their equivalent widths. The atomic line data used in deriving the chemical composition are given in Table 1.

3.3. Abundances

From the above analysis we find: $T_{\rm eff}$=6500 K, $\log g = 0.5$, $\xi_t = 5$ km s^{-1}, and a metallicity of [M/H]=-1.0. Abundances derived using the above model are given in Table 2.

The abundance of Li has been determined by spectrum synthesis (Fig. 3) analysis of Li I resonance doublet feature at 6707.8 Å. The basic line data required for the synthetic spectrum has been taken from Lambert et al. (1993). From the spectrum synthesis analysis of the Li-feature, we derive an upper limit to Li-abundance of IRAS 05341+0852: $\log \epsilon$(Li)=2.5. We derived the carbon abundance both from spectrum synthesis and line analysis using the lines at 6587.6Å, 7111.5Å, 7113.2Å, 7115.2Å and 7119.6Å. The internal scatter among the individual carbon lines is very small. For N I we have three features at 7423.6 Å, 7442.2 Å, and 7468.3 Å. The line at 7442.2 Å is not used in our analysis, as it is affected by cosmic ray event. The line at 7423.6 Å is blended with the Si I and the abundance derived from this line is $\log \epsilon$ (N) = 8.50. The clean N I line at 7468.27 Å yields an abundance of $\log \epsilon$ (N)= 8.04 which is 0.5 dex less than that obtained from N I line at 7423.63 Å.

We derive oxygen abundance by spectrum synthesis of the O I triplet at 7774 Å and O I triplet at 6156Å. The O I lines at 7774Å are very strong and these are known to be plagued by non-LTE effects. The derived average abundance from the three lines at 7774Å is $\log \epsilon$(O I)=9.2 dex. From the studies of non-LTE effects on the triplet by Takeda (1994), we approximately derived the abundance difference of $\Delta \log \epsilon$ (O I) $\leq$ 0.8 between LTE and non-LTE analysis. This analysis yields an oxygen abundance of [O/H] = -0.5.

From an analysis O I triplet at 6156Å in the WHT spectra, we derive an abundance of $\log\epsilon$(O I)=8.5 dex ([O/H] = -0.4), which is adopted in our discussion.

Table 1. Line data: Wavelength (λ_{lab}), low excitation potential (LEP), equivalent width (EW), derived abundance (log ϵ), log gf and reference for the gf values. Abundances are derived using a model atmosphere: T_{eff}= 6500K, log g=0.5, ξ_t=5 km s^{-1} and [M/H]=-1.0

λ_{lab}	LEP	EW	log ϵ	log gf	Ref.	λ_{lab}	LEP	EW	log ϵ	log gf	Ref.
Li I			≤2.25*			Fe II					
6707.754	0.00			-0.43	a	6147.786	3.89	76	6.45	-2.92	d
6707.766	0.00			-0.21	a	6149.236	3.89	96	6.58	-2.88	d
6707.904	0.00			-0.73	a	6369.463	2.89	52	6.70	-4.31	d
6707.917	0.00			-0.51	a	6456.391	3.90	178	6.73	-2.25	d
C I						6516.083	2.89	110	6.47	-3.55	d
6587.622	8.53	103	8.53	-1.22	b	Ni I					
7111.480	8.64	132	9.02	-1.32	b	5709.555	1.68	36	5.55	-1.90	d
7113.180	8.64	176	9.00	-0.93	b	6256.367	1.68	36	5.72	-2.09	d
7115.190	8.64	160	8.83	-0.90	b	6643.638	1.68	12	5.35	-2.01	d
7116.990	8.64	180	9.20	-1.08	b	6767.784	1.83	25	5.43	-1.89	d
7119.660	8.64	130	8.99	-1.31	b	7393.609	3.61	26	5.17	-0.04	d
N I						7422.286	3.63	50	5.55	-0.01	d
7423.630	10.33	60	8.50	-0.61	b	7525.118	3.63	24	5.80	-0.69	d
7468.271	10.33	60	8.04	-0.13	b	7555.607	3.85	53	5.71	0.06	d
O I			9.2*			Y II					
7771.954	9.14			0.33	b	5480.761	1.72	168	2.93	-1.00	d
7774.177	9.14			0.19	b	5728.872	1.84	160	3.21	-1.21	d
7775.395	9.14			-0.03	b	6795.410	1.74	112	3.03	-1.58	d
Al I						6858.240	1.74	110	2.54	-1.11	d
6696.032	3.14	30	6.85	-1.67	d	Ba II					
6698.670	3.14	31	7.14	-1.95	d	5853.688	0.60	395	3.62	-0.92	d
Si II						6496.908	0.60	475	3.19	-0.07	d
6347.090	8.12	280		0.26		La II					
6371.350	8.12	227		-0.05		6399.049	2.63	120	3.26	-0.65	e
S I			6.31*			6642.790	2.51	64	3.07	-1.08	e
6757.007	7.87			-0.83	c	6834.050	0.24	104	3.45	-3.19	e
6757.171	7.87			-0.24	c	Ce II					
6757.195	7.87			-0.24	c	5512.062	1.01	150	2.25	0.20	d
Ca I						5610.246	1.05	130	2.31	0.00	d
6102.727	1.88	70	5.64	-0.80	d	5668.916	1.01	155	2.60	-0.11	d
6122.226	1.89	124	5.54	-0.20	d	6043.400	1.21	63	2.02	-0.17	d
6439.083	2.52	95	5.67	-0.05	d	Pr II					
6449.800	2.52	25	5.40	-0.62	d	5810.622	1.43	30	1.76	-0.65	f
6717.690	2.71	50	5.74	-0.39	d	5879.253	1.35	33	1.32	-0.24	f
Sc II						6200.790	1.35	17	1.46	-0.74	f
6245.620	1.51	90	2.37	-1.15	d	6397.960	1.04	57	1.90	-0.82	f
6604.600	1.36	115	2.52	-1.23	d	Nd II					
Fe I						5842.385	1.28	158	2.73	-0.34	d
5586.771	3.37	132	6.59	-0.12	d	6365.385	0.93	46	2.45	-1.41	g
6136.620	2.45	84	6.63	-1.40	d	Sm II					
6137.702	2.59	72	6.64	-1.35	d	6256.660	1.16	62	1.69	-1.63	f
6230.735	2.56	89	6.60	-1.24	d	6502.000	1.55	63	2.39	-1.97	f
6335.337	2.20	35	6.66	-2.20	d	6569.224	1.49	125	1.81	-0.89	f
6336.830	3.69	30	6.37	-0.68	d	6570.670	0.99	60	1.78	-1.91	f
6400.010	3.60	113	6.57	-0.07	d	6741.474	0.99	75	1.74	-1.72	f
6411.658	3.65	60	6.54	-0.49	d	7039.225	0.99	101	1.68	-1.45	f
6421.360	2.28	50	6.74	-2.01	d	7051.520	0.92	76	1.51	-1.56	f
6494.994	2.40	126	6.79	-1.24	d	Eu II					
6592.926	2.72	38	6.56	-1.60	d	6437.698	1.32	60	0.65	0.05	d
6677.999	2.69	75	6.56	-1.60	d	6645.127	1.38	75	1.13	-0.25	d
7411.162	4.28	52	6.84	-0.33	d						
7445.758	4.26	69	6.70	-0.02	d						
7495.077	4.22	102	6.78	0.18	d						
7511.031	4.18	70	6.30	0.32	d						

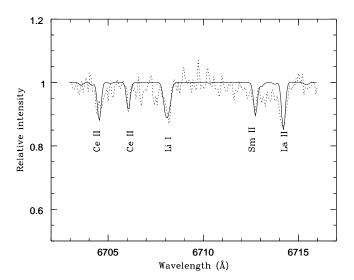Note:- (a) Lambert et al (1993); (b) Lambert et al (1982); (c) Biemont et al (1993) (d) Thevenin (1989,1990)
(e) Bord et al (1996); (f) Kurucz &Peytremann (1975),(g) Ward (1985)
*: these values are derived from spectrum synthesis

Table 2. Abundance analysis of IRAS 05341+0852. The values in the brackets are: T$_{eff}$, log g and microturbulent velocity. Solar photosphere abundances (log $\epsilon_\odot$) are taken from Grevesse and Noels (1993)

Element	# of lines	log $\epsilon_\odot$	Model (6500 K, 0.5, 5 km s^{-1}) log ϵ	σ	[el/H]	Model (6000 K, 1.0, 5 km s^{-1}) log ϵ	σ	[el/H]	Model (5500 K, 1.0, 5 km s^{-1}) log ϵ	σ	[el/H]
Li I	1	1.16	≤2.5		1.3	≤2.0		0.9	≤1.6		0.5
C I	6	8.55	8.92	0.22	0.36	9.12	0.22	0.56	8.72	0.22	0.16
			8.77*								
N I	2	7.97	8.27		0.30	8.65		0.68	7.62		-0.35
O I	2	8.87	8.5*		-0.37	8.9		0.03	9.4		0.53
Al I	2	6.47	6.93		0.46	6.66		0.19	6.08		-0.39
Si II	2	7.55	7.98		0.43	8.32		0.77	8.63		1.08
S I	1	7.21	6.51*		-0.70						
Ca I	5	6.36	5.59	0.13	-0.77	5.22	0.14	-1.14	4.94	0.15	-1.42
Sc II	2	3.17	2.44		-0.63	2.37		-0.80	2.21		-0.89
Fe I	16	7.50	6.62	0.14	-0.88	6.18	0.15	-1.32	5.60	0.38	-1.90
Fe II	5		6.59	0.12	-0.91	6.54	0.12	-0.96	6.62	0.14	-0.88
Ni I	8	6.25	5.53	0.21	-0.72	5.07	0.17	-1.18	4.31	0.42	-1.94
Y II	4	2.24	2.93	0.28	0.69	2.85	0.29	0.61	2.69	0.29	0.45
Ba II	3	2.13	3.44	0.22	1.31	3.03	0.30	0.90	2.79	0.30	0.66
La II	3	1.22	3.26	0.19	2.04	3.18	0.12	1.96	3.02	0.10	1.80
Ce II	4	1.55	2.29	0.24	0.74	2.18	0.23	0.63	1.96	0.23	0.42
Pr II	4	0.71	1.63	0.26	0.92	1.52	0.26	0.81	1.33	0.25	0.62
Nd II	2	1.50	2.59		1.09	2.46		0.90	2.22		0.72
Sm II	7	1.01	1.81	0.28	0.8	1.6	0.12	0.59	1.59	0.35	0.58
Eu II	2	0.51	0.89		0.38						

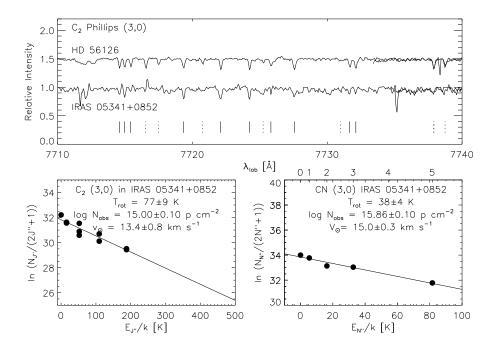Note:- *: these values are derived from spectrum synthesis analysis

Fig. 3. Spectrum synthesis fit for IRAS 05341 in the Li and Al region. The solid line corresponds to observed spectrum and the dashed line represents the spectrum synthesized for the abundances: [Fe/H]= −0.88 and log ε (Li)= 2.5.

The abundance of sulphur has been derived from spectrum synthesis of S I lines at 6757 Å. Abundance of aluminum [Al/Fe]=1.36 is based on the two weak Al I lines at 6696.03Å and 6698.66Å. We derived the abundance of Si ([Si/Fe]=1.33) from Si II line at 6371.767 Å (the Si II line at 6347 Å is

blended). Our abundance analysis of Fe is based on 14 Fe I and 7 Fe II lines.

The abundance of light s-process element Y is found to be large with respect to Fe ([Y/Fe]=1.59). Ba abundance may be uncertain by at least 0.3 to 0.4 dex because it is based on two strong lines with an equivalent width ≥ 400 mÅ. The abundances of other major heavy s-process elements La ([La/Fe]=2.94) and Ce ([Ce/Fe]=1.64) clearly demonstrates that IRAS 05341 is in fact rich in s-process elements. The other heavy elements like Pr, Nd, and Sm also show large overabundances. The spectrum of IRAS 05341 is well dominated by strong Nd II lines. However we were able to deduce the Nd abundance ([Nd/Fe]=2.0) from only two Nd II lines due to scarcity of atomic data for other lines. The abundance of Sm ([Sm/Fe]=1.70) is derived from 7 Sm II lines and the abundance of Pr ([Pr/Fe]=1.82) is based on four Pr II lines. We found overabundance of r-process element Eu (Eu II/Fe=1.3) in IRAS 05341. The abundance of Eu has been derived from two Eu II lines at 6437.69Å and 66451.13Å.

The internal scatter in the derived abundances of each element having more than two lines is represented by standard deviation (σ) in Table 2. The internal scatter (σ) in the abundances may be due to uncertainties in gf values and in measured equivalent widths. The uncertainties in the derived atmospheric parameters are: $T_{\rm eff}$: $\pm$ 250 K, log g: $\pm$ 0.5, and ξ_t: $\pm$1 km s^{-1} and the uncertainties in the derived abundances are: Fe: $\pm$0.3 dex, Li: $\pm$0.3 dex, C, N, and O: $\pm$0.1 dex, and s-process elements: $\pm$0.2 dex. We have also derived abundances using relatively cooler models : T$_{eff}$=6000 K, log g=1.0 and ξ_t= 5 km s^{-1} and

Fig. 4. Upper panel: the C_2 Phillips (3,0) band in the spectra of HD 56126 and IRAS 05341+0852. The solid vertical lines are the identified lines used in the absolute rotational diagram, and the dotted vertical lines mark the position of molecular lines note detected. Lower panels: the absolute rotational diagram of the C_2 Phillips (3,0) and CN Red system bands of IRAS 05341+0852.

T_{eff}=5500 K, log g=1.0 and ξ_t=5 km s^{-1} (Table 2). The abundance analysis with cooler models also shows overabundances of Li, CNO, Al, and s-process elements. The small σ value of Fe I abundances and the difference between Fe I and Fe II abundances for a model atmosphere: T_{eff}= 6500 K, log g=0.5 and ξ_t=5 km s^{-1} suggest that this adopted model best represents the photosphere of IRAS 05341. We have also checked abundance calculations using recent line-blanketed model atmospheres of Kurucz (1992, private communication). The results obtained from both Kurucz and MARCS model atmospheres are in good agreement within the uncertainties quoted above.

3.4. Circumstellar molecular absorption lines

IRAS 05341 shows the C_2 Phillips and CN Red System bands in absorption (Fig. 3). Since the S/N of the spectra is 40, only the strongest molecular features are identified. Furthermore the CN (3,0) band is in a part of the spectrum which exhibits many telluric absorption features. An analysis of the C_2 $A^1\Pi_u - X^1\Sigma_g^+$ (3,0) and CN $A^2\Pi - X^2\Sigma^+$ (3,0) bands as described in Bakker et al. (1996a,b) has been made. The molecular constants used and the method applied for analysis are extensively described in their papers. For C_2 (3,0) we find $v_\odot$ = 13.4 ± 0.8 km s^{-1}, T_{rot} = 77 ± 9 K, and log N = 15.00 ± 0.10 p cm^{-2}, and for CN (3,0) $v_\odot$ = 15.0 ± 0.4 km s^{-1}, T_{rot} = 38 ± 4 K, and log N = 15.86 ± 0.10 p cm^{-2}. The velocities are heliocentric. C_2 has no permanent dipole moment and behaves suprathermally, while CN (with dipole moment) behaves subthermally. Since only the lowest J'' and N'' lines are used in the analyses, the C_2 temperature is not as high as one might expect, nor is the CN temperature that low.

From the difference between the velocity of the molecular lines and the velocity of the photospheric atomic lines (v_r =

25 km s^{-1}) we find an expansion velocity of the AGB ejecta of v_{exp} = 10.8 ± 1.0 km s^{-1}.

All stars exhibiting the unidentified 21 μm feature show C_2 and CN in absorption (Bakker et al. 1996a,b). The rotational temperature, column density, and expansion velocity found for this star are of the same order as those of the other stars and clearly point to the fact that these lines are formed in the circumstellar shells around these post-AGB stars. Since C_2 Phillips and CN Red System bands have been detected in this object we also expect to see the C_2 Swan, the CN Violet System, and possible the C_3 Swing bands in absorption.

4. Discussion

The overabundances of s-process elements and carbon in IRAS 05341 is a direct evidence for the association of s-process enhancements with shell-flashes and dredge-up. These are likely responsible for the increase in C/O. The most likely neutron source is ^{13}C. The small amounts of hydrogen get mixed with ^{12}C rich material which is just below the hydrogen burning shell due to semi convection during He-shell flashes (Hollowell & Iben 1988). This hydrogen reacts with ^{12}C resulting in ^{13}C. When ^{13}C enriched matter is mixed down due to He-shell flash, it burns via the reaction ^{13}C(α, n)^{16}O which generates neutrons for s-process elemental production. This reaction is quite efficient, requiring temperatures ≤1.5× 10^8 K, which are easily found in the inter-shell convective zone of models of low-mass stars. Models indicate that this is more efficient in metal-poor AGB stars and/or post-AGB stars with small envelope mass (Iben & Renzini 1984, Lattanzio 1989). The s-process enrichment in the atmosphere of IRAS 05341 presumably has taken place during the shell flash events on the AGB. Also the r-process element Eu has been found to be overabundant relative to Fe. The [Eu/Fe]

ratio is similar to that found in metal-poor population II stars (Sneden & Parthasarathy 1983).

Using the Tables of Malaney (1987), a mean neutron exposure $(\tau_o) = 0.3$, assuming exponential distribution of neutron exposure, is suggested. This is about half the value found by Gonzalez & Wallerstein (1994) for the post-AGB stars ROA 24 and V1 in Omega Centauri.

The overabundance of Li and Al in IRAS 05341 could indicate that there was Hot Bottom Burning (HBB), where the base of the convective envelope is hot enough for nucleosynthesis to occur (Lattanzio 1993). HBB has been suggested as the mechanism responsible for the production of Li in the Li-rich AGB stars (Wood et al. 1983, Smith and Lambert 1989). In fact these are bright AGB stars which are oxygen-rich rather than carbon-rich. Recent calculations by Sackmann and Boothroyd (1992) showed that Li-rich and O-rich AGB stars are the result of HBB. In the HBB models temperatures of the order of $0.5 - 1 \times 10^8$ K are encountered at the base of the convective envelope (Blöcker and Schönberner 1991, Lattanzio 1992). This is hot enough for the reaction $^{25}Mg(p,\gamma)$ ^{26}Al resulting in the production of Al. More recent model calculations of HBB in AGB stars by Lattanzio et al. (1996) and Mowlavi (1995) show that significant amount of Li and Al are convected to the surface as a result of third dredge-up and HBB. Also, it is possible, when HBB is shut down due to mass-loss the recurring third dredge-up may yet produce a carbon star (Lattanzio et al. 1996).

The Cameron-Fowler mechanism or the Beryllium transport mechanism can explain the production of Li. However the models show that it takes place more efficiently in most massive AGB stars. The models indicate that HBB may not take place in low-mass AGB stars (Lattanzio et al 1996, Mowlavi 1995). The overabundance of Li and Al in IRAS 05341, is an important issue to be understood, as its metallicity (Fe/H=-1.0), high galactic latitude, post-AGB evolutionary stage and luminosity indicate that it is a low-mass evolved star belonging to an old disk or halo population group of stars. It is a puzzle how a low-mass star can produce Li and Al, if it has not gone through the HBB. Recently Abia et al. (1993) found that 2% of the galactic carbon stars are super-rich Li stars, for which the masses are estimated to lie between 1 and 2 $M_\odot$. The presence of Li in these stars is still a mystery. From its low-mass nature and overabundance of Li and C, IRAS 05341 is found to be the successor of the Li-rich carbon stars.

5. Conclusions

Based on an analysis of high resolution spectra of of IRAS 05341 we adopt the atmospheric parameters: T_{eff}=6500 K, $\log g$=0.5, ξ_t = 5 km s^{-1} and [M/H]=-1.0. We found the star to be metal-poor ([Fe/H])=-0.9. The radial velocity v_r = 25 km s^{-1} and its large displacement ($\approx$ 2 kpc) from the Galactic plane indicate that it may belong to old disc population. The study of chemical composition and its molecular spectra yield the following quantitative results:

1. Overabundances of C ([C/Fe]=1.26) and N ([N/Fe]=1.2) indicate that both H- and He- burning products are brought onto the surface by dredge-ups on the AGB.

2. Large overabundance of s-process elements (Y, Ba, La, Ce, Sm etc) indicate that star has gone through third dredge-up episodes. The amount of s-process enhancement is similar to that seen in Fg Sge.

3. The overabundance of Li ([Li/Fe]$\leq$2.5) and Al ([Al/Fe]=1.4) in IRAS 05341 is a puzzle. Further chemical composition analysis of several carbon-rich post-AGB stars may shed some light on this issue.

4. Circumstellar C_2 and CN has been detected in absorption at an expansion velocity of $v_{exp} = 10.8 \pm 1.0$ km s^{-1}. This confirms that all 21 μm objects shows these molecules (Bakker et al. 1996b). For C_2 (3,0), we find $v_\odot$ = 13.4 $\pm$ 0.8 km s^{-1}, T_{rot} = 77 $\pm$ 9 K, and $\log N$ = 15.00 $\pm$ 0.10 p cm^{-2}, and for CN (3,0) $v_\odot$ = 15.0 $\pm$ 0.4 km s^{-1}, T_{rot} = 38 $\pm$ 4 K, and $\log N$ = 15.86 $\pm$ 0.10 p cm^{-2}. C_2 behaves superthermal and CN subthermal.

References

Abia, C., Boffin, H.M.J., Isern, J., Rebolo, R. 1993, A&A 272, 445
Bakker, E.J., Waters, L.B.F.M., Lamers, H.J.G.L.M., Trams, N.R., van der Wolf, F.L.A.: 1996a, A&A 310, 893
Bakker, E.J., van Dishoeck, E.F., Waters, L.B.F.M., Schoenmaker, T. 1996b, A&A in press
Biemont, E., Quinet, P., Zeippen, C.J. 1993, A&AS, 102, 435
Blöcker, T., Schönberner, D. 1991, A&A 244, L43
Bord, D.J., Barisciano, L.P., Jr. Cowley, C.R. 1996, MNRAS 278, 997
Flower, J.J. 1977, A&A 54, 31
Geballe, T.R. & van der Veen, W.E.C.J. 1990, A&A 235, L9
Gonzalez, G. & Wallerstein, G. 1994, AJ 108, 1325
Grevesse, N., Noels, A. 1992, in " Origin and evolution of the elements " ed. N. Prantzos., E. Vangioni-Flam & M. Casse (Cambridge, Univ. press), 15
Gustafsson, B., Bell, R.A., Eriksson, K., and Nordlund, A. 1975, A&A 42, 407
Hrivnak, B.J. 1995, ApJ 438,341
Hollowell, D. & Iben, I.Jr. 1988, ApJ 333, L25
Iben, I. Jr. & Renzini, A. 1984, Phys. Rep. 105, 329
Kipper, T. & Kipper, M. 1993, A&A 276, 389
Klochkova, V.G. 1995, MNRAS 272,710
Kurucz, L.R. 1979, ApJS 40, 1
Kurucz, L.R. & Peytremann, E. 1975, SAO Spec.Rep. No. 362
Kwok, S., Hrivnak, B.J., Boreiko, R.T. 1987, ApJ 312, 303
Kwok, S., Hrivnak, B.J., Geballe, T.R. 1995, ApJ 454, 394
Lambert, D.L., Roby, S.W., Bell, R.A. 1982, ApJ 254, 664
Lambert, D.L., Smith, V.V., Heath, J. 1993, PASP 105, 568
Lattanzio, J.C. 1989, ApJ 344, L25
Lattanzio, J.C. 1992, Proc. Astron. Soc. Aust. 10, 120

Lattanzio, J.C. 1993, IAU Symposium 155 on "Planetary Nebulae", P. 235, edited by R. Weinberger and A.Acker

Lattanzio, J.C., et al. 1996, IAU Symposium 177 on " The Carbon Star Phenomenon" edited by R. Wing (in press)

McCarthy, J.K., Sandiford, B.A., Boyd, D., Booth, J. 1993, PASP 105, 881

Malaney, R.A. 1987, Ap&SS 137, 251

Manchado, A., Pottasch, S.R., Garcia-Lario, P., Esteban, C., Mampaso, A. 1989, A&A 214,139

Mowlavi, N., 1995, In Proc. ESO/EIPC Workshop " The Light Elements Abundances " Springer, P. 297

Omont, A., Loup, C., Forveille, T., Te Lintel Hekkert, P., Habing, H., Sivagnanam, P. 1993, A&A 267, 515

Parthasarathy, M. & Pottasch, S.R. 1986, A&A 154, L16

Parthasarathy, M., Garcia Lario, P., Pottasch, S.R. 1992, A&A 264, 159

Parthasarathy, M. 1993, ASP conf. Ser 45, on "Luminous High Latitude Stars ", P. 173 edited by D. Sasselov

Pottasch, S.R. & Parthasarathy, M. 1988, A&A 192, 182

Reddy, B.E. & Parthasarathy, M. 1996, AJ 112, 2053

Sackmann, I.-J. & Boothroyd, A.I. 1992, ApJ 392, L71

Smith, V.V. & Lambert, D.L. 1989, ApJ 345, L75

Sneden, C. 1973, Ph.D. thesis, University of Texas

Sneden, C., Parthasarathy, M. 1983, ApJ 267, 757

Takeda, Y. 1994, PASJ 46, 53

Thévenin, F. 1989, A&AS 77, 137

Thévenin, F. 1990, A&AS 82, 179

van Winckel, H., Waelkens, C., Waters, L.B.F.M. 1996, A&A 306, L37

Ward, L. 1985, MNRAS 213, 71

Wood, P.R., Bessel, M.S., Fox, M.W. 1983, ApJ 272, 99